Journal of Medicinal Chemistry

Article

1,2,4-Triazolo-[1,5-a]pyridine HIF Prolylhydroxylase Domain-1 (PHD-1) Inhibitors With a Novel Monodentate Binding Interaction

Saleh Ahmed, Andrew Ayscough, Greg R Barker, Hannah E. Canning, Richard Davenport, Robert Downham, David Harrison, Kerry Jenkins, Natasha Kinsella, David G. Livermore, Susanne Wright, Anthony David Ivetac, Robert Skene, Steven J. Wilkens, Natalie A. Webster, and Alan G. Hendrick

J. Med. Chem., **Just Accepted Manuscript** • Publication Date (Web): 08 Jun 2017

ACS Publications

Journal of Medicinal Chemistry is published by the American Chemical Society. 1155 Sixteenth Street N.W., Washington, DC 20036

1,2,4-Triazolo-[1,5-a]pyridine HIF Prolylhydroxylase Domain-1 (PHD-1) Inhibitors With a Novel Monodentate Binding Interaction

Saleh Ahmed,[†] *Andrew Ayscough,*[†] *Greg R. Barker,*[†] *Hannah E. Canning,*[†] *Richard Davenport,*[†] *Robert Downham,*[†] *David Harrison,*[†] *Kerry Jenkins,*[*,†] *Natasha Kinsella,*[†] *David G. Livermore,*[†] *Susanne Wright,*[†] *Anthony D. Ivetac,*[‡] *Robert Skene,*[‡] *Steven J. Wilkens,*[‡] *Natalie A. Webster*[¥] *and Alan G. Hendrick.*[¥]

† Department of Medicinal Chemistry, Takeda Cambridge Ltd., 418 Cambridge Science Park, Milton Road, Cambridge, CB4 0PZ, United Kingdom

ǂ Department of Computational Sciences & Crystallography, Takeda California Inc., 10410 Science Center Dr, San Diego, CA 92121, United States

¥ Department of in vitro Pharmacology, Takeda Cambridge Ltd., 418 Cambridge Science Park, Milton Road, Cambridge, CB4 0PZ, United Kingdom

ABSTRACT: Herein we describe the identification of 4-{[1,2,4]triazolo[1,5-a]pyridin-5-yl}benzonitrile based inhibitors of the hypoxia-inducible factor prolylhydroxylase domain-1 (PHD-1) enzyme. These inhibitors were shown to possess a novel binding mode by X-ray crystallography, in which the triazolo N1 atom coordinates in a hitherto unreported monodentate interaction with the active site Fe^{2+} ion, whilst the benzonitrile group accepts a hydrogen bonding interaction from the side chain residue of

Asn315. Further optimization led to potent PHD-1 inhibitors with good physicochemical and pharmacokinetic properties.

Introduction. Hypoxia-inducible factors (HIFs) are heterodimeric transcription factors comprising of an alpha subunit (HIF-1α, HIF-2α or HIF-3α) and a beta subunit (HIF-1β, HIF-2β or HIF-3β). HIFs, and in particular HIF-1α, have been shown to be master regulators of oxygen homeostasis in response to limited oxygen environments.[1] Multiple target genes have been identified with the main downstream effects being to increase anaerobic respiration *via* stimulation of the glycolytic pathways,[2] to improve tissue oxygenation by enhancing vascularisation (angiogenesis),[3] and increasing red blood cell production (erythropoiesis).[4] In normoxic environments HIF-1 is negatively regulated by hydroxylation of the α-subunit and subsequent proteosomal degradation *via* the von Hippel-Lindau (VHL) - E3 ubiquitin ligase system.[5] The hydroxylation of HIFs are mediated by prolylhydroxylase domain enzymes (PHDs) which are non-heme iron(II) dependent enzymes of which there are three catalytically competent isoforms (PHD-1, 2 & 3).[6] The PHD enzymes utilise 2-oxoglutarate (2-OG) and molecular oxygen as substrates and hence in oxygen depleted environments (i.e. hypoxia) their ability to mediate HIF turnover is diminished resulting in HIF stabilisation, binding to hypoxia response elements (HRE) and gene activation. Despite the active site across the PHD isoforms being highly conserved, the different isoforms appear to perform some distinct as well as overlapping roles. This can be attributed in part to differential expression and localisation but also due to subtle differences in substrate specificities.[6f]

There is increasing interest in exploring pharmacological intervention of the HIF-PHD axis in a variety of disease settings due to its key role in ischemia and inflammation, such as in inflammatory bowel disorders (e.g. Ulcerative Colitis, Crohn's disease),[7] ischemic reperfusion injuries (cardiac,[8] cerebrovascular,[9] liver [10] and renal [11]) and neurodegenerative processes. [12] Other potential clinical

settings include anemia,[13] wound healing and organ transplantation.[14] There have been extensive efforts towards the development of small molecule inhibitors of PHD enzymes.[15] Direct pharmacological inhibitors of PHDs fall into four categories: (1) Fe^{2+} substitutes (e.g. Co^{2+}, Ni^{2+} and Cu^{2+}); (2) Fe^{2+} sequesters (e.g. desferrioxamine, L-mimosine etc.); (3) 2-OG mimetics (e.g. dimethyloxalylglycine and *N*-oxalyl-D-phenylalanine); and (4) targeted active-site inhibitors (e.g. Roxadustat (formerly FG-4592),[16] N-{[5-(3-chlorophenyl)-3-hydroxy-2-pyridinyl]carbonyl}glycine (Vadadustat, formerly AKB-6548),[17] 2-[6-(4-morpholinyl)-4-pyrimidinyl]-4-(1H-1,2,3-triazol-1-yl)-1,2-dihydro-3H-pyrazol-3-one (Molidustat, formerly BAY 85-3934)[18] etc.). Clearly the scope for development and use of iron substitutes, sequesters and 2-OG mimetics for clinical use are severely hampered by the lack of specificity over a multitude of off-target metabolic systems. Targeting the PHD active site gives far more scope for specific and selective modulation of PHDs/HIFs, however it is a notable facet of the majority of inhibitors reported to date that chelation binding to the active-site ferrous ion plays a significant role in driving ligand potency. This has non-trivial consequences from a molecular properties standpoint that may limit the potential for some of these compounds as *in vivo* tool compounds and as potential drug candidates.

Results and Discussion. A fragment screening campaign identified triazolopyrimidine **1** as a moderately potent inhibitor of PHD-1 (7.1μM) with a reasonably good ligand efficiency[19] of 0.30 (Figure 1.). We were intrigued by the relative simplicity of the architecture of this hit and by its structural divergence from other PHD inhibitor motifs seen internally and in the literature.[15] Initially, we sought to investigate the key requirements for binding through systematic deletion of the heterocyclic core nitrogen atoms. Removal of one of the 5-membered rings' non-bridgehead nitrogen atoms (compound **2**) resulted in a 3-fold drop in potency, suggesting this nitrogen might be making a modest binding interaction. Deletion of the other non-bridgehead nitrogen from the 5-membered ring

(compound **3**) abolished potency demonstrating that this atom has a key role in binding. Conversely, removal of the non-bridgehead nitrogen from the 6-membered ring (compound **4**) actually improved potency ~10-fold to 0.67μM (L.E. 0.36). In view of the promising lead-like potential of this compound we decided to continue optimization on the 1,2,4-triazolo-[1,5-a]pyridine scaffold.

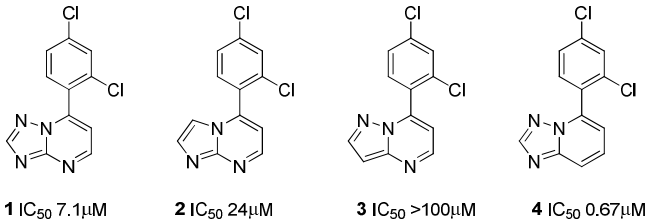

Figure 1. Initial fragment lead and exploratory core SAR.

Keeping the core triazolo[1,5-a]pyridine constant, we sought to investigate the SAR of the phenyl 'top ring' by conducting a positional scan of simple substituents (Table 1.). The SAR showed a preference for electron withdrawing substituents in the 4-position. In particular, the *para*-nitrile compound, **17**, displayed a significant increase in potency and binding efficiency (0.034μM, L.E. 0.44).

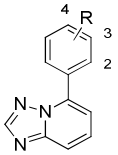

Table 1. SAR of 'Top Ring'

	R	PHD-1 IC_{50} (μM)
5	H	30
6	4-Cl	0.55
7	3-Cl	26

8	2-Cl	48
9	4-F	1.3
10	3-F	28
11	2-F	24
12	4-Me	5.6
13	3-Me	>100
14	4-OMe	26
15	3-OMe	55
16	2-OMe	>100
17	4-CN	0.034
18	3-CN	61

X-Ray Crystallography: Crystal structures of ligands bound to PHD-2 are prevalent in the literature, but until now, no PHD-1 crystal structures have been reported. During the course if our investigation we obtained a 2.5Å resolution X-ray crystal structure of **17** bound into PHD-1 using a co-crystallization method (Figure. 2).

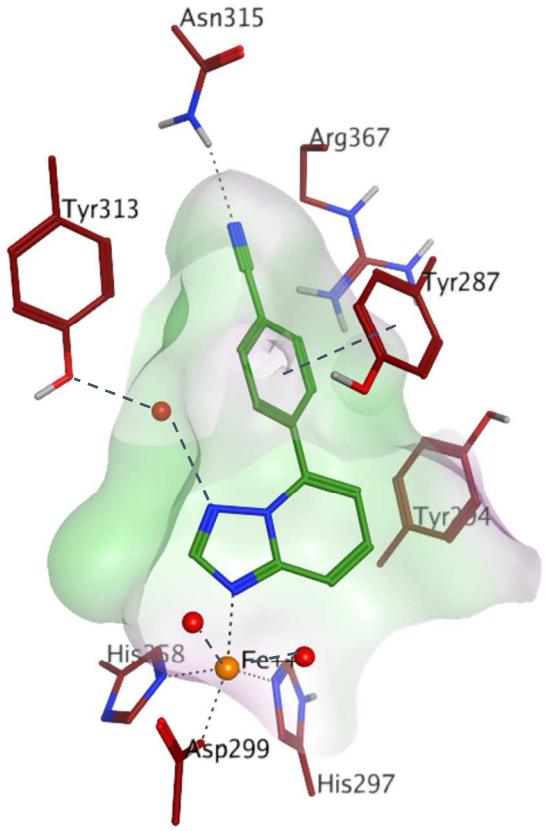

Figure 2. X-ray crystal structure of **17** bound in the active site of PHD-1 (PDB accession code 5V1B).

This showed a number of interesting features (Figure 2 and 3), most notably a monodentate coordination of the triazolopyridine N1-atom with the active site Fe^{2+} ion. To date, virtually all reported competitive PHD inhibitors are shown (or are postulated) to make a bidentate chelation interaction to iron. It has been proposed through computational docking that the PHD-2 inhibitor 6-amino-1,3-dimethyl-5-[(2-pyridinylsulfanyl)acetyl]-2,4(1H,3H)-pyrimidinedione (TM6089) coordinates in a non-chelation fashion although this has not been substantiated by experimental methods.[9a] To the best of our knowledge this is the first verified example of a monodentate-iron binding PHD inhibitor. The significance of this is that many chelation binders invoke highly polar or ionisable moieties, such as amides, phenols and hydroxyl groups. The physicochemical properties of such groups (e.g. pK_a, PSA) often runs counter to desirable drug-like chemical space, especially for CNS indications where crossing the blood-brain barrier presents a significant hurdle to achieving efficacious drug concentrations.[20]

Other noteworthy features include the benzonitrile moiety that projects into the protein inducing the formation of an 'Arg367-out' pocket with the nitrile group accepting a hydrogen bond interaction from the side chain of Asn315. Many reported PHD inhibitors target Arg367 (Arg383 in PHD-2 structures) *via* a carboxylate or similarly acidic residue – again, moieties that are often not ideal for oral exposure. Additionally, the phenyl ring is positioned appropriately to make a π-stacking interaction with Tyr287 and the triazolopyridine N3 atom is potentially making a water-mediated interaction to Tyr313.

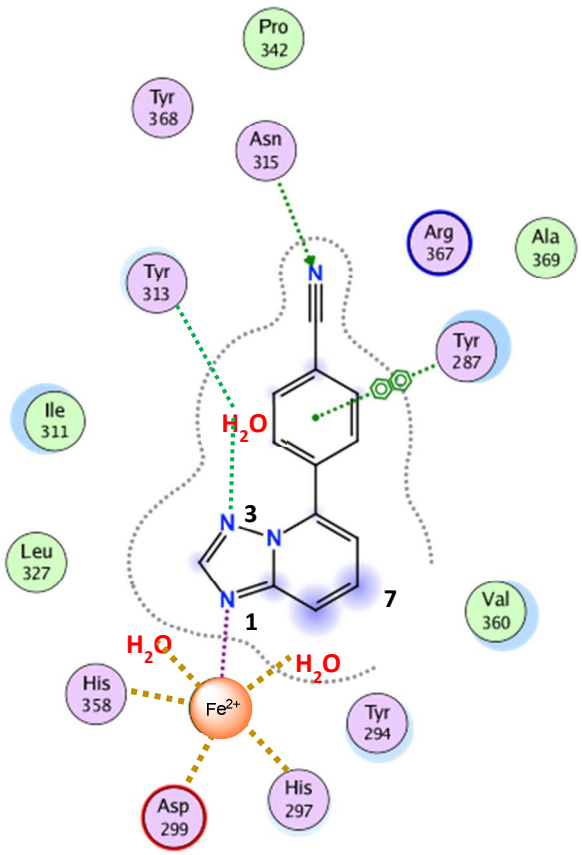

Figure 3. Ligand interaction diagram of **17** bound in the active site of PHD-1.

The crystal structure suggests that there is very limited scope for extending substituents from all but the 7-position of the triazolopyridine bicyclic scaffold and that substitution of the benzonitrile 'top ring' may be restricted to small substituents. These assertions were in agreement with the observed SAR (Table 2). Although the focus of our research led us to optimize our series against the PHD-1 isoform

we also generated a crystal structure of **17** bound into PHD-2 (PDB accession code 5V18, not shown) which showed essentially the same key binding features. This is unsurprising given the identity of the active site region between PHD-1 and PHD-2, and consistent with the observation that PHD-1 activity broadly tracked PHD-2 activity for these compounds (data not shown).

Core Bicyclic SAR: Introduction of a methyl group at C2 resulted in >15-fold drop in potency (**19**). Similarly, an amino substituent at C2 lost 10-fold potency relative to **17** and further N-methylation or N-acylation substantially diminished potency. Incorporation of a methyl substituent at C8 was barely tolerated and even a fluorine substituent resulted in >250-fold drop off in potency. The former is consistent with the steric constraints conferred by the binding of N1 to iron and the latter we speculate is due to the electronic effects of fluorine making N1 a weaker coordinating atom. In the case of the original triazolopyrimidine hit (**1**) it is probable that both N-atoms are chelating to iron but in doing so are presenting the 'top ring' in a sub-optimal orientation for additional beneficial interactions.

The C6 position could only accommodate small substituents (F, Me, NH_2) with 10 to 20-fold drop off in potency, anything larger abolished potency. As predicted by the crystal structure, C7 was tolerant of a variety of substituents with similar or improved potencies relative to **17**. The vector from this position leads out of the protein into solvent space, and towards a flexible loop region. This suggested that opportunities for significant new binding interactions may be limited. Nonetheless, this position became our main focus for tuning potency and optimizing the physicochemical properties of the series (*vide infra*).

Top Ring SAR: The position *ortho* to the nitrile group supported fluorine substituents with good levels of potency but anything larger abruptly diminished potency. The *meta* positions were slightly more accommodating, with fluorine, methyl and amino retaining potency and chlorine and methoxy showing only a small drop-off, within 4-fold of **17**. Interestingly, CF_3 was not tolerated suggesting steric considerations alone do not explain the SAR and that electronics may also play an important role.

Combinations of fluorine atoms (*o* and *m* positions) and methyl groups (*m* positions) were generally well tolerated although di-*meta* substituted compounds were generally less active than mono-substituted analogues.

In addition to exploring substituents on the top ring we sought to investigate heterocyclic replacements with a view to altering properties such as lowering lipophilicity, increasing solubility and increasing fractional sp^3 character (Table 3). We found that introducing nitrogen atoms *ortho* to the nitrile resulted in modest drops in potency relative to the benzonitrile analogue (**55**, 5-fold and **56**, 2.5-fold). However, heteroaromatics containing nitrogen atoms in the *meta* position relative to the nitrile had more pronounced drop-offs in potency (**57**, 8-fold, **58**, 38-fold and **59**, 40-fold), especially when combined with an *ortho* nitrogen. None of the 5-membered heteroaromatic top ring replacements showed any appreciable inhibition against PHD-1. This is unsurprising given the directional requirements of the nitrile to making an efficient hydrogen bond with Asn315 whilst maintaining the N1 interaction with iron. We did however observe some potency with saturated 6-membered heterocyclic replacements. The cyano piperidine **64**, showed 0.28μM potency whilst piperazine cyanamide was 1.8μM. Molecular modeling shows that these ligands are able to adopt conformations that allow good binding interactions to both Asn315 and iron, but that either the increased volume due to the sp^3 hybridisation, or the loss of the π-π interaction is detrimental to binding. The saturated cyano pyrrolidino and 2-azaspiro[3.3]heptanes examples were not significantly active.

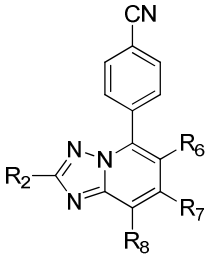

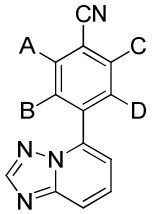

Table 2. SAR of Core Bicycle and Top Ring.

	R_2	R_8	R_7	R_6	A	B	C	D	PHD-1 IC_{50} (μM)
19	Me								0.57
20	NH_2								0.24
21	NMe_2								18
22	NHAc								2.5
23		F							9.6
24		Me							80
25			Me						0.039
26			NH_2						0.013
27			NHEt						0.025
28			NHAc						0.008
29				F					0.46
30				Me					0.46
31				NH_2					0.77
32				NMe_2					>10

33	NHAc					>10
34		F				0.010
35		Me				0.83
36		CF_3				1.87
37		Cl				3.9
38			F			0.050
39			Me			0.074
40			Et			6.1
41			NH_2			0.057
42			NHAc			>10
43			Cl			0.14
44			OMe			0.14
45			CF_3			>10
46		F		F		0.034
47		F	F			0.067
48			F		F	0.16
49		F	Me			0.052
50			Me	F		0.14

51		Me	F	0.22
52		Me	Me	0.20
53	NH_2	Me		0.09
54	NHAc	Me		0.07

Table 3. Cyano-Heterocyclic Top Rings.

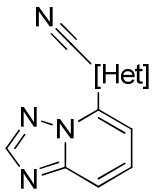

	[Het]	PHD-1 IC_{50} (μM)		[Het]	PHD-1 IC_{50} (μM)
55	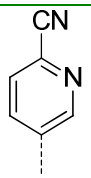	0.17	**61**	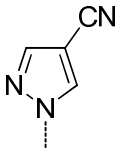	>10
56	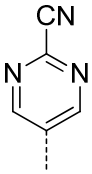	0.084	**62**	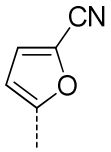	>10
57	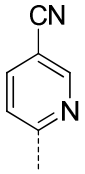	0.27	**63**	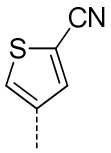	>10
58	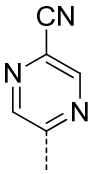	1.28	**64**	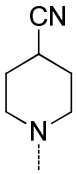	0.28

59	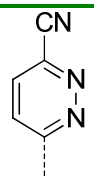	1.37	**65**	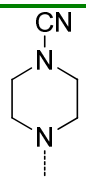	1.8
60	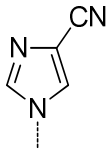	>10	**66**	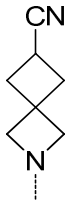	>10
			67	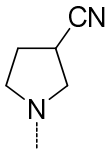	>10

Table 4. Mouse Pharmacokinetic Profiles of Selected Compounds.

		AUC_{0-t} (ng.h/mL)[a]	Cmax (μm)[a]	F%	Cl (mL/min/kg)[b]	%PPB (mu)	B/P	$K_{p,uu}$	MDR1 efflux[c]	cLogP	PSA	Kinetic Sol. (μM)	PAMPA (nm/s)
17	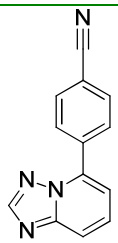	176	0.80	40	108	71.3	0.95	1.11	0.8	2.59	54	44	246
39	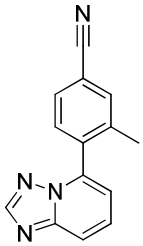	1869	5.58	100	31.6	79.0	0.88	1.59	0.68	3.10	54	189	409
53	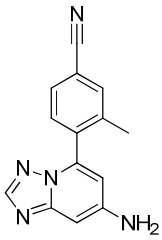	40038	14.8	39	0.48	69.8	0.21	0.39	12	2.27	80	151	59

54	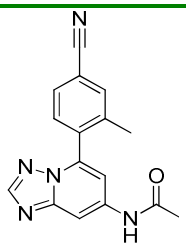	3658	5.00	100	17.5	51.4	0.03	0.02	99	2.34	83	99	29

a Cassette PK, male C57BL6 mice, dosed 3 mg/kg p.o. in 0.5% methylcellulose. b Cassette PK, male C57BL6 mice, dosed 0.5 mg/kg i.v. in DMA:Saline (50:50). c Absorption Systems ExpressPlus BBB penetration potential determined using MDR1-MDCK cell monolayers.

Pharmacokinetic profiles: The early lead compound **17** was found to have modest oral exposure in mouse largely driven by high clearance (Table 4). This compound showed a moderate rate of microsomal turnover *in vitro* (data not shown) which in part explains the high *in vivo* clearance. Comparable brain exposure levels were seen ($K_{p,uu}$ 1.11 and B/P 0.95) suggesting that this series could be amenable to optimization for CNS indications if peripheral exposure levels could be enhanced. Accordingly, incorporation of a methyl group in the *meta* position of the 'top ring' (**39**) improved oral exposure whilst maintaining good levels of CNS penetration. In addition to reducing clearance through improved microsomal stability we observed that the methyl group improves both the solubility and permeability presumably by reducing the planarity of the molecule via the axial twist that this substituent imparts. The SAR data and crystal structure had shown that the 7-position was amenable to modification, so we optimised substituents at this position to tailor physicochemical and ADME properties. For example, the introduction of a 7-amino group (**53**) was found to dramatically enhance peripheral exposure by further reducing clearance. This might be attributed to the lowering of LogP or it could be masking a metabolic soft-spot. Although **53** exhibits excellent peripheral exposure, the compound does not partition well into the brain ($K_{p,uu}$ 0.39 and B/P 0.21). Similarly the 7-N-acetamide (**54**) exhibits reasonable peripheral exposure but poor brain levels ($K_{p,uu}$ 0.02 and B/P 0.03). Both of these

compounds have high PSA and they have reduced solubility and permeability relative to the 7-H analogue (**39**). It is well known that these factors impact a molecule's ability to cross the blood-brain barrier. In addition to adverse physicochemical properties for CNS penetration, these compounds were shown to be substrates for MDR1 in an *in vitro* MDCK-MDR1 assay (efflux ratios 12 and 99 respectively) suggesting that active efflux from the CNS could be a major contributor to reduced CNS levels of free drug.

Scheme 1. General Synthetic Routes to 1,2,4-Triazolo-[1,5-a]pyridines

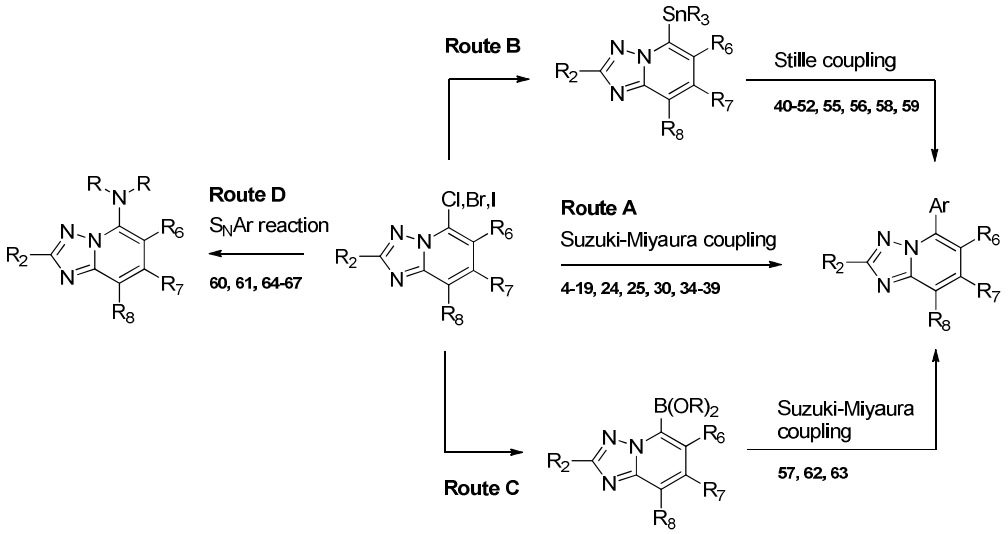

Scheme 2. Preparation of 5-Halo-1,2,4-triazolo-[1,5-a]pyridine Intermediates

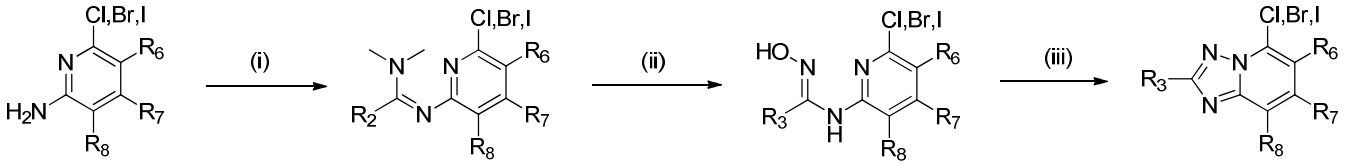

(i) R_2-C(OMe)$_2$NMe$_2$, 70 – 110 °C, 1.25 – 12 h, EtOH or IPA or toluene; (ii) HONH$_2$.HCl, rt – 50 °C, 1 – 2 h, IPA or MeOH; (iii) TFAA or Eaton's reagent, 0.33 – 18 h, rt – 105 °C, THF.

Scheme 3. Synthetic Routes to 7-Amino Analogues

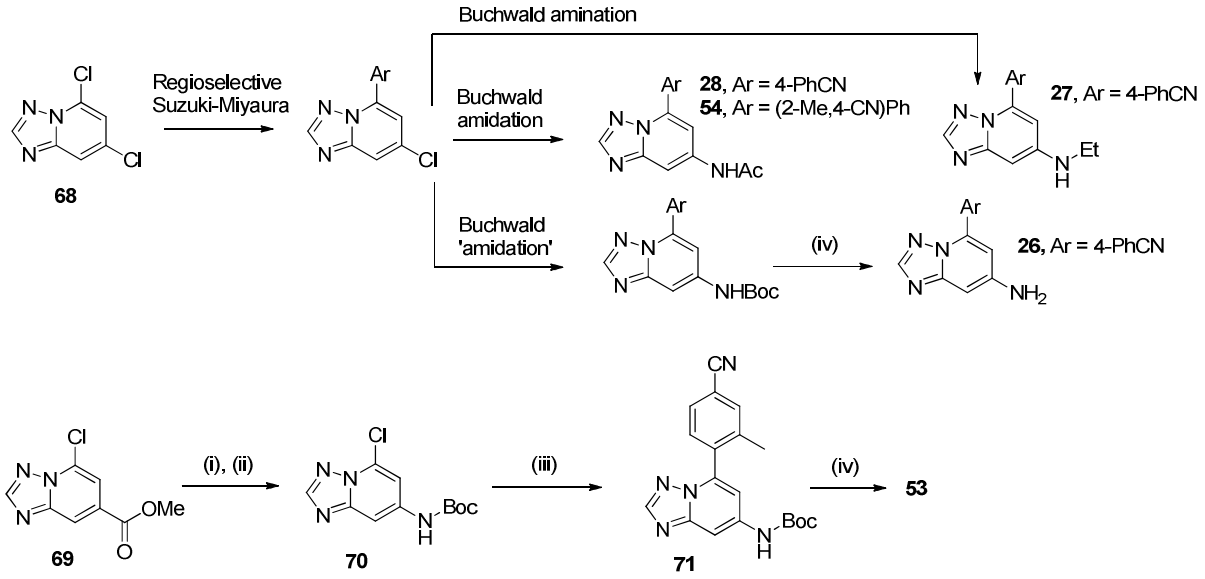

(i) 2M (aq.) LiOH, rt, 1 h, THF/MeOH (1:1); (ii) $(PhO)_2PON_3$, Et_3N, 0.5 h, *t*-BuOH, 90 °C, toluene; (iii) (4-cyano-2-methylphenyl)boronic acid, $PdCl_2$(dppf), Na_2CO_3, 100 °C, 2 h, 1,4-dioxane/water (5:1); (iv) HCl, 50 °C, 2 h, 1,4-dioxane.

Chemistry. The majority of compounds were accessed *via* corresponding 5-halo-1,2,4-triazolo-[1,5-a]pyridines using one of four routes (Scheme 1): direct Suzuki-Miyaura coupling (route A); [21] conversion to the tri-*n*-butyl or trimethyl stannane followed by Stille coupling (route B); [22] conversion to a boronic acid derivative followed by Suzuki-Miyaura coupling (route C) and direct S_NAr displacement (route D). In cases where the 5-halo-1,2,4-triazolo-[1,5-a]pyridines were not commercially available the scaffolds were typically synthesised from corresponding 2-amino-6-halopyridines whereby the aminopyridine was condensed with a dimethylamide dimethyl acetal and then treated with hydroxylamine hydrochloride. The hydroxyamidine was cyclised under dehydrating conditions (e.g. TFAA or Eaton's reagent) to give the corresponding 5-halo-1,2,4-triazolo-[1,5-a]pyridine (Scheme 2).[23] In the cases of 7-amino substituted compounds the amino group could be introduced in a couple of ways (Scheme 3). Starting from the 5,7-dichloro intermediate (**68**), accessed using the previously described route, the aryl ring could be installed by regioselective Suzuki-Miyaura reaction at the 5-position. The 7-chloro

could then be displaced under Buchwald-Hartwig[24] amination conditions to give 7-alklyamino products (e.g. **27**) or by using modified Buchwald 'amidation' conditions[25] to give 7-aminoacyl compounds (e.g. **28**). Similarly, these modified Buchwald conditions could be used to prepare 7-N-*tert*-butoxycarbonylamino intermediates that could be deprotected to 7-amino compounds (e.g. **26**). Alternatively, the 5-chloro-7-carboxylic ester intermediate (**69**), accessed using the previously described route, could be converted to the 7-N-*tert*-butoxycarbonylamino intermediate (**70**) using a Curtius rearrangement. Subsequent Suzuki-Miyaura coupling and deprotections for example, gave **53**.

Conclusion. We have identified a novel series of potent PHD-1 inhibitors and we report the first PHD-1 isoform X-ray crystal structure with one of our lead compounds bound in to the active site. The structural data shows that this chemotype operates through a unique monodentate binding interaction with the active site iron in concert with other key interactions accessed via an induced 'Arg367-out' pocket. The observed SAR is consistent with many of the features revealed by the X-ray crystal structure. Unlike many of the reported PHD inhibitors this scaffold is highly amenable to optimization for good oral exposure, both peripherally and in the CNS making these useful tool compounds to study *in vivo* pharmacological effects of PHD enzyme inhibition and for further evaluation as potential drug candidates.

Experimental Section. The synthesis of key compounds is described below. Full experimental procedures for the synthesis of all other compounds are described in the supplementary information.

General Procedures. All solvents and chemicals were used as purchased without further purification. The progress of all reactions was monitored on Waters ZQ-2000 system UPLC systems. Ultra Performance Liquid Chromatography (UPLC) with UV (photodiode array) detection over a wide range of wavelengths, normally 220-450 nm, using a Waters (trade mark) Acquity UPLC system equipped with Acquity UPLC BEH, HSS or HSS T3 C18 columns (2.1mm id x 50mm long) operated at 50 or 60 °C. Mobile phases typically consisted of acetonitrile mixed with water containing either 0.1% formic acid, 0.1% TFA or 0.025% ammonia. Mass spectra were recorded with a Waters SQD single quadrupole mass spectrometer using atmospheric pressure ionization. Proton (^{1}H) NMR spectra were recorded on a Bruker Avance 400 or a Bruker Avance 300 using deuterated solvents specified in the experiments. Chemical shifts are given in parts per million (ppm) (δ relative to residual solvent peak). Preparative HPLC was performed using Agilent Technologies 1100 Series system or a Waters autopurification LC/MS system or a Shimadzu semi prep HPLC system, typically using Waters 19 mm id x 250 mm long C18 columns such as XBridge™ or SunFire™ 5 µm materials at room temperature. Mobile phases typically consisted of acetonitrile mixed with water containing either 0.1% formic acid or 0.1% ammonia, unless otherwise stated. Super Critical Fluid Chromatography (SFC) chiral separations were performed on a Waters prep 30/MS system, using a flow rate of 30 mL/min, temperature of 40 °C and a pressure of 100 bar. Mobile phases typically consisted of supercritical CO_2 and a polar solvent such as methanol, ethanol or isopropanol. Column type and eluent are detailed for individual examples. All final compounds were determined to be >95% purity by LC/MS.

4-{[1,2,4]Triazolo[1,5-a]pyridin-5-yl}benzonitrile (17). A stirred suspension of 5-bromo-[1,2,4]triazolo[1,5-a]pyridine [CAS 143329-58-2] (2.00 g, 10.10 mmol), (4-cyanophenyl)boronic

acid [CAS 126747-14-6] (1.484 g, 10.10 mmol), tetrakis(triphenylphosphine)palladium(0) (0.817 g, 0.707 mmol) and cesium carbonate (3.95 g, 12.12 mmol) in 1,4-dioxane (28 mL) and water (5.6 mL) was placed under an inert atmosphere with 3 x N_2/vacuum cycles. The reaction was heated to 100 °C for 3 hrs. The reaction was diluted with EtOAc whilst hot and was filtered through Celite, washing with further amounts of EtOAc. The filtrate was concentrated *in vacuo*. The crude product was recrystallized from hot EtOH to afford 4-{[1,2,4]triazolo[1,5-a]pyridin-5-yl}benzonitrile (**17**) as a white solid (909 mg, 4.13 mmol, 45%). ^{1}H NMR (400 MHz, DMSO-d_6) δ ppm 7.49 - 7.53 (m, 1 H), 7.78 - 7.84 (m, 1 H), 7.94 - 7.98 (m, 1 H), 8.05 - 8.10 (m, 2 H), 8.20 - 8.25 (m, 2 H), 8.58 (s, 1 H), MS ES$^+$: 221

3-Methyl-4-{[1,2,4]triazolo[1,5-a]pyridin-5-yl}benzonitrile (39). A suspension of 5-bromo-[1,2,4]triazolo[1,5-a]pyridine [CAS 143329-58-2] (1.75 g, 8.81 mmol), (4-cyano-2-methylphenyl)boronic acid [CAS 313546-18-8] (1.56 g, 9.69 mmol), $PdCl_2$(dppf) (0.65 g, 0.881 mmol) and sodium carbonate (1.87 g, 17.62 mmol) in 1,4-dioxane (24 mL) and water (4.9 mL) was flushed with N_2 and heated to 100 °C for 1h. The reaction was cooled and partitioned between EtOAc and water. The organic phase was collected, washed with brine, dried (phase separator) and concentrated *in vacuo*. The resulting residue was purified by flash chromatography (0-70% EtOAc in petroleum ether on basic silica). The appropriate fractions were collected and concentrated *in vacuo*. The resulting residue was recrystallized from hot EtOH to afford 3-methyl-4-{[1,2,4]triazolo[1,5-a]pyridin-5-yl}benzonitrile (**39**) as a white solid (991 mg, 4.23 mmol, 48%). ^{1}H NMR (400 MHz, DCM-d_2) δ ppm 2.19 (s, 3 H), 7.05 (d, J = 7.07 Hz, 1 H), 7.54 (d, J = 7.83 Hz, 1 H), 7.64 - 7.77 (m, 3 H), 7.85 - 7.92 (m, 1 H), 8.33 (s, 1 H), MS ES$^+$: 235

4-[7-Amino-[1,2,4]triazolo[1,5-a]pyridin-5-yl]-3-methylbenzonitrile (53). A solution of methyl 2-amino-6-chloropyridine-4-carboxylate [CAS 1005508-80-4] (10.0 g, 53.6 mmol) and DMF-DMA (7.18 mL, 53.6 mmol) was heated to 70 °C for 2h. More DMF-DMA (7.18 mL, 53.6 mmol) was added and the reaction was heated for a further 4h. The reaction was cooled to 50 °C and hydroxylamine hydrochloride (3.72 g, 53.6 mmol) was added. The reaction was stirred at 50 °C for 2h. The reaction was concentrated *in vacuo* and the resulting residue was triturated with EtOH. The precipitate was filtered and dried under vacuum to afford methyl 2-chloro-6-(N'-hydroxyformimidamido)isonicotinate (12.0 g, 98%). ^{1}H NMR (400 MHz, DMSO-d_6) δ ppm 3.32 (s, 3 H), 7.24 (d, J = 1.14 Hz, 1 H), 7.59 (d, J = 1.14 Hz, 1 H), 7.72 (d, J = 9.73 Hz, 1 H), 10.02 (d, J = 9.73 Hz, 1 H), 10.37 - 10.43 (m, 1 H), MS ES$^+$: 230

A solution of methyl 2-chloro-6-(N'-hydroxyformimidamido)isonicotinate (12.0 g, 52.3 mmol) in THF (105 mL) was treated with TFAA (14.8 mL, 105 mmol). The reaction was heated to 40 °C for 18h. The reaction was quenched and basified with saturated (aq) $NaHCO_3$ and partitioned between EtOAc and water. The organic was collected, dried (phase separator) and concentrated *in vacuo*. The resulting residue was purified by flash chromatography (0-100% EtOAc in petroleum ether on SiO_2) to afford methyl 5-chloro-[1,2,4]triazolo[1,5-a]pyridine-7-carboxylate (**69**) (6.44g, 58%). ^{1}H NMR (400 MHz, MeOH-d_4) δ ppm 4.03 (s, 3 H), 7.88 (d, J = 1.52 Hz, 1 H), 8.43 (d, J = 1.52 Hz, 1 H), 8.66 (s, 1 H), MS ES$^+$: 212.

A solution of methyl 5-chloro-[1,2,4]triazolo[1,5-a]pyridine-7-carboxylate (**69**) (6.44 g, 30.4 mmol) in methanol (51 mL) and THF (51 mL) was treated with LiOH (2M aq) (30.4 mL, 60.9 mmol). The reaction was stirred at room temperature for 1h. The reaction was acidified with 2N HCl (30 mL) and the resulting precipitate was filtered, washed with MeOH and dried to afford 5-

chloro-[1,2,4]triazolo[1,5-a]pyridine-7-carboxylic acid (5.15 g, 86%). ^{1}H NMR (400 MHz, DMSO-d_6) δ ppm 7.79 (d, J = 1.52 Hz, 1 H), 8.35 (d, J = 1.39 Hz, 1 H), 8.79 (s, 1 H), 13.98 (br. s., 1 H), MS ES$^+$: 198

A suspension of 5-chloro-[1,2,4]triazolo[1,5-a]pyridine-7-carboxylic acid (1.00 g, 5.06 mmol) in toluene (15 mL) was treated sequentially with TEA (1.058 mL, 7.59 mmol), *tert*-butanol (0.484 mL, 5.06 mmol) and diphenyl phosphorazidate (1.091 mL, 5.06 mmol). The reaction was heated to 90 °C under N_2 for 30 min. The reaction was concentrated *in vacuo* and the resulting residue was purified by flash chromatography (0-100% EtOAc in petroleum ether on SiO_2) to afford *tert*-butyl (5-chloro-[1,2,4]triazolo[1,5-a]pyridin-7-yl)carbamate (**70**) (1.02 g, 75%). ^{1}H NMR (400 MHz, DCM-d_2) δ ppm 1.53 (s, 9 H), 6.94 - 7.06 (m, 1 H), 7.39 (d, J = 2.02 Hz, 1 H), 7.68 (d, J = 2.02 Hz, 1 H), 8.25 (s, 1 H), MS ES$^+$: 213

A suspension of *tert*-butyl (5-chloro-[1,2,4]triazolo[1,5-a]pyridin-7-yl)carbamate (**70**) (0.200 g, 0.744 mmol), (4-cyano-2-methylphenyl)boronic acid [CAS 313546-18-8] (120 mg, 0.744 mmol), $PdCl_2$(dppf) (54.5 mg, 0.074 mmol) and sodium carbonate (158 mg, 1.489 mmol) in 1,4-dioxane (2 mL) and water (0.400 mL) was flushed with N_2 and heated to 100 °C for 2h. The reaction was cooled to room temperature and partitioned between EtOAc and water. The organic was collected, washed with brine, dried (phase separator) and concentrated *in vacuo*. The resulting residue was purified by flash chromatography (0-100% EtOAc in petroleum ether on basic silica) to afford *tert*-butyl (5-(4-cyano-2-methylphenyl)-[1,2,4]triazolo[1,5-a]pyridin-7-yl)carbamate (194 mg, 75%). ^{1}H NMR (400 MHz, DMSO-d_6) δ ppm 1.52 (s, 9 H), 2.10 (s, 3 H), 7.15 - 7.23 (m, 1 H), 7.61 - 7.74 (m, 1 H), 7.82 - 7.90 (m, 1 H), 7.92 - 8.02 (m, 2 H), 8.31 (s, 1 H), 10.10 (s, 1 H), MS ES$^+$: 294 (M-^{t}Bu).

A solution of *tert*-butyl (5-(4-cyano-2-methylphenyl)-[1,2,4]triazolo[1,5-a]pyridin-7-yl)carbamate (0.194 g, 0.555 mmol) and HCl (4M in 1,4-dioxane) (0.694 mL, 2.78 mmol) in 1,4-dioxane (5 mL) was heated to 50 ℃ for 2h. The reaction was concentrated *in vacuo* and the resulting residue was purified by SCX-2 cationic exchange cartridge, loading and washing with MeOH and eluting with 2M NH_3 in MeOH. The resulting residue was purified by reverse phase preparative HPLC eluted with acetonitrile / water (with 0.1% ammonia) to afford 4-(7-amino-[1,2,4]triazolo[1,5-a]pyridin-5-yl)-3-methylbenzonitrile (**53**) as a white solid (77 mg, 0.303 mmol, 54.5 % yield). ^{1}H NMR (400 MHz, DCM-d_2) δ ppm 2.18 (s, 3 H), 4.39 (br. s., 2 H), 6.40 (d, J = 2.15 Hz, 1 H), 6.83 (d, J = 2.27 Hz, 1 H), 7.47 (d, J = 7.83 Hz, 1 H), 7.59 - 7.69 (m, 2 H), 8.01 (s, 1 H) MS ES$^+$: 250

N-[5-(4-Cyano-2-methylphenyl)-[1,2,4]triazolo[1,5-a]pyridin-7-yl]acetamide (54). DMF-DMA (5.13 mL, 38.3 mmol) was added to a solution of 4,6-dichloropyridin-2-amine [CAS 116632-24-7] (5.00 g, 30.7 mmol) in EtOH (150 mL). The reaction was heated to 85 °C for 75 mins. The reaction mixture was allowed to cool to room temperature then solvent was removed *in vacuo* to give N'-(4,6-dichloropyridin-2-yl)-N,N-dimethylmethanimidamide as a brown oil which was taken on to the next step without purification. Hydroxylamine hydrochloride (2.99 g, 43.0 mmol) was added to a solution of N'-(4,6-dichloropyridin-2-yl)-N,N-dimethylmethanimidamide (6.70 g, 30.7 mmol) in MeOH (133 mL) under nitrogen. The reaction was stirred at room temperature for 1 h and then concentrated *in vacuo*. The residue was triturated with water and the solid collected by filtration, washing with water. The solid was dried under vacuum overnight to afford N-(4,6-dichloropyridin-2-yl)-N'-hydroxymethanimidamide (6.12 g, 97 %). ^{1}H NMR (400 MHz, DMSO-d_6) δ ppm 7.13 (s, 2 H) 7.68 (d, J = 10 Hz, 1 H) 9.89 (d, J = 10 Hz, 1 H) 10.44 (s, 1 H).

(N-(4,6-Dichloropyridin-2-yl)-N'-hydroxymethanimidamide (6.12 g, 29.7 mmol) and Eaton's reagent (30 mL) were combined and heated to 105 °C for 20 min. The reaction mixture was allowed to cool to room temperature, diluted with ice water and basified with solid K_2CO_3 to pH 8. The resulting solution was extracted twice with EtOAc, and the organic layers were combined and dried over $MgSO_4$, filtered, and concentrated *in vacuo*. The residue was recrystallized from MTBE to afford 5,7-dichloro-[1,2,4]triazolo[1,5-a]pyridine (**68**) (4.63 g, 83%). ^{1}H NMR (300 MHz, DMSO-d_6) δ ppm 7.76 (d, J = 2 Hz, 1 H) 8.16 (d, J = 2 Hz, 1 H) 8.66 (s, 1 H), MS ES$^+$: 188.

A suspension of 5,7-dichloro-[1,2,4]triazolo[1,5-a]pyridine (**68**) (2.00 g, 10.6 mmol), (4-cyano-2-methylphenyl)boronic acid (1.79 g, 11.13 mmol), tetrakis(triphenylphosphine)palladium(0) (0.61 g, 0.53 mmol) and Na_2CO_3 (0.888 g, 8.38 mmol) in DME (80 mL) and water (16 mL) was de-gassed and refilled with N_2. The reaction was heated to reflux for 2h. The reaction was poured into water and extracted twice with EtOAc. The organics were combined, dried (phase separator) and concentrated *in vacuo*. The resulting residue was purified by flash chromatography (0-100% EtOAc in petroleum ether on basic silica) to afford 4-(7-chloro-[1,2,4]triazolo[1,5-a]pyridin-5-yl)-3-methylbenzonitrile (1.6 g, 57%). ^{1}H NMR (400 MHz, DMSO-d_6) δ ppm 2.12 (s, 3 H), 7.46 (d, J = 1.83 Hz, 1 H), 7.70 (d, J = 7.94 Hz, 1 H), 7.87 (d, J = 7.63 Hz, 1 H), 7.96 (s, 1 H), 8.22 (d, J = 2.14 Hz, 1 H), 8.53 (s, 1 H), MS ES$^+$: 269.

A solution of 4-(7-chloro-[1,2,4]triazolo[1,5-a]pyridin-5-yl)-3-methylbenzonitrile (0.250 g, 0.930 mmol), acetamide (0.110 g, 1.861 mmol), cesium carbonate (0.606 g, 1.861 mmol), $Pd_2(dba)_3$ (0.043 g, 0.047 mmol) and dicyclohexyl(2',4',6'-triisopropyl-[1,1'-biphenyl]-2-yl)phosphine (0.044 g, 0.093 mmol) in 1,4-dioxane (4 mL) was degassed with nitrogen for 5 mins. The reaction mixture was heated in a sealed vial at 110 °C for 1.5 hours. The reaction was

removed from heating and allowed to cool, diluted in EtOAc (30 mL), washed with water (10 mL) and brine, dried ($MgSO_4$) and concentrated *in vacuo*. The crude product was absorbed onto Celite and purified by column chromatography on basic silica, eluted with 0-100% [9:1 EtOAc/MeOH]/petroleum ether. The resulting residue was further purified by reverse phase preparative HPLC eluted with acetonitrile / water (with 0.1% ammonia) to afford N-(5-(4-cyano-2-methylphenyl)-[1,2,4]triazolo[1,5-a]pyridin-7-yl)acetamide (**54**) as a white solid (46.8 mg, 0.161 mmol, 17% yield). ^{1}H NMR (400 MHz, DMSO-d_6) δ ppm 2.11 (s, 3 H) 2.15 (s, 3 H) 7.20 (d, J = 2 Hz, 1 H) 7.67 (d, J = 8 Hz, 1 H) 7.86 (d, J = 8 Hz, 1 H) 7.94 (s, 1 H) 8.23 (d, J = 2 Hz, 1 H) 8.35 (s, 1 H) 10.56 (s, 1 H), MS ES$^+$: 292.

ASSOCIATED CONTENT

Supporting Information

Contains PHD-1 activity assay protocols; PAMPA and MDR1-MDCK-pgp efflux protocols; synthetic procedures and analytical data for all novel compounds (in Microsoft Word file format). Compound SMILES strings and associated activity and ADME data (in csv file format).

This material is available free of charge via the Internet at http://pubs.acs.org

Accession Codes

PDB code for PHD-1 bound with **17** is 5V1B and for PHD-2 bound with **17** is 5V18. Authors will release the atomic coordinates and experimental data upon article publication.

AUTHOR INFORMATION

Corresponding Author

* Phone, +44 (0)1223 336 427; E-mail: drkerryjenkins@yahoo.co.uk

Present Address

* Wren Therapeutics Ltd., c/o University of Cambridge, Department of Chemistry, Lensfield Road, Cambridge, United Kingdom, CB2 1EW.

Author Contributions

All authors have given approval to the final version of the manuscript.

ACKNOWLEDGMENT

We would like to acknowledge the contributions from Michael Bestwick for stimulating discussion on pharmacokinetics, and Johannes Grosse for his support and guidance throughout this program. Also we would like to thank Mark Portsmouth (analytical), Suzi Cowan (NMR), Paul Strutt (HPLC/UPLC) and Divya Lad (PAMPA) for their support and hard work.

X-Ray crystallographic images and 2D interaction diagram generated using Molecular Operating Environment (MOE), 2013.08; Chemical Computing Group Inc., 1010 Sherbooke St. West, Suite #910, Montreal, QC, Canada, H3A 2R7, 2016.

ABBREVIATIONS

2-OG, 2-oxoglutarate; B/P, Brain / Plasma ratio; CAS, Chemical Abstracts Service registry number; dba, dibenzylideneacetone; DMF-DMA, dimethylformamide-dimethyl acetal; dppf, 1,1'-bis(diphenylphosphino)ferrocene; Eaton's reagent, 7.7 wt% phosphorus pentoxide solution in methanesulfonic acid; ES, electrospray ionization; EtOAc, ethyl acetate; EtOH, ethanol; Het, heterocycle; HIF, Hypoxia-Inducible Factor; HRE, Hypoxia Response Elements; IPA, Isopropyl alcohol; $K_{p,uu}$, unbound brain-to-plasma concentration ratios; MDCK, Madin-Darby canine

kidney; MDR1, Multidrug Resistance Protein 1; PHD, Prolylhydroxylase Domain; pK_a, logarithmic acid dissociation constant; SCX-2, silylated propyl phosphonic acid Strong Cationic Exchange Resin; S_NAR, nucleophilic aromatic substitution; Sol., Solubility; TEA, triethylamine; VHL, von Hippel-Lindau.

REFERENCES

1. (a) Bacon, N. C.; Wappner, P.; O'Rourke, J. F.; Bartlett, S. M.; Shilo, B.; Pugh, C. W.; Ratcliffe, P. J. Regulation of the Drosophila bHLH-PAS protein Sima by hypoxia: functional evidence for homology with mammalian HIF-1 alpha. *Biochem. Biophys. Res. Commun.* **1998,** *249* (3), 811-816; (b) Maxwell, P. H.; Pugh, C. W.; Ratcliffe, P. J. Inducible operation of the erythropoietin 3' enhancer in multiple cell lines: evidence for a widespread oxygen-sensing mechanism. *Proc. Natl. Acad. Sci. U. S. A.* **1993,** *90* (6), 2423-2427; (c) Semenza, G. L.; Wang, G. L. A nuclear factor induced by hypoxia via de novo protein synthesis binds to the human erythropoietin gene enhancer at a site required for transcriptional activation. *Mol. Cell. Biol.* **1992,** *12* (12), 5447-5454.

2. (a) Iyer, N. V.; Kotch, L. E.; Agani, F.; Leung, S. W.; Laughner, E.; Wenger, R. H.; Gassmann, M.; Gearhart, J. D.; Lawler, A. M.; Yu, A. Y.; Semenza, G. L. Cellular and developmental control of O_2 homeostasis by hypoxia-inducible factor 1 alpha. *Genes Dev.* **1998,** *12* (2), 149-162; (b) Seagroves, T. N.; Ryan, H. E.; Lu, H.; Wouters, B. G.; Knapp, M.; Thibault, P.; Laderoute, K.; Johnson, R. S. Transcription factor HIF-1 is a necessary mediator of the pasteur effect in mammalian cells. *Mol. Cell. Biol.* **2001,** *21* (10), 3436-3444.

3. (a) Carmeliet, P.; Dor, Y.; Herbert, J. M.; Fukumura, D.; Brusselmans, K.; Dewerchin, M.; Neeman, M.; Bono, F.; Abramovitch, R.; Maxwell, P.; Koch, C. J.; Ratcliffe, P.; Moons, L.;

Jain, R. K.; Collen, D.; Keshert, E. Role of HIF-1alpha in hypoxia-mediated apoptosis, cell proliferation and tumour angiogenesis. *Nature* **1998,** *394* (6692), 485-490; (b) Kelly, B. D.; Hackett, S. F.; Hirota, K.; Oshima, Y.; Cai, Z.; Berg-Dixon, S.; Rowan, A.; Yan, Z.; Campochiaro, P. A.; Semenza, G. L. Cell type-specific regulation of angiogenic growth factor gene expression and induction of angiogenesis in nonischemic tissue by a constitutively active form of hypoxia-inducible factor 1. *Circ. Res.* **2003,** *93* (11), 1074-1081; (c) Ryan, H. E.; Lo, J.; Johnson, R. S. HIF-1 alpha is required for solid tumor formation and embryonic vascularization. *EMBO J.* **1998,** *17* (11), 3005-3015.

4. Yu, A. Y.; Shimoda, L. A.; Iyer, N. V.; Huso, D. L.; Sun, X.; McWilliams, R.; Beaty, T.; Sham, J. S.; Wiener, C. M.; Sylvester, J. T.; Semenza, G. L. Impaired physiological responses to chronic hypoxia in mice partially deficient for hypoxia-inducible factor 1alpha. *J. Clin. Invest.* **1999,** *103* (5), 691-696.

5. (a) Huang, L. E.; Gu, J.; Schau, M.; Bunn, H. F. Regulation of hypoxia-inducible factor 1alpha is mediated by an O_2-dependent degradation domain via the ubiquitin-proteasome pathway. *Proc. Natl. Acad. Sci. U. S. A.* **1998,** *95* (14), 7987-7992; (b) Kallio, P. J.; Wilson, W. J.; O'Brien, S.; Makino, Y.; Poellinger, L. Regulation of the hypoxia-inducible transcription factor 1alpha by the ubiquitin-proteasome pathway. *J. Biol. Chem.* **1999,** *274* (10), 6519-6525; (c) Salceda, S.; Caro, J. Hypoxia-inducible factor 1alpha (HIF-1alpha) protein is rapidly degraded by the ubiquitin-proteasome system under normoxic conditions. Its stabilization by hypoxia depends on redox-induced changes. *J. Biol. Chem.* **1997,** *272* (36), 22642-22647.

6. (a) Bruick, R. K.; McKnight, S. L. A conserved family of prolyl-4-hydroxylases that modify HIF. *Science* **2001,** *294* (5545), 1337-1340; (b) Chowdhury, R.; Leung, I. K.; Tian, Y.

M.; Abboud, M. I.; Ge, W.; Domene, C.; Cantrelle, F. X.; Landrieu, I.; Hardy, A. P.; Pugh, C. W.; Ratcliffe, P. J.; Claridge, T. D.; Schofield, C. J. Structural basis for oxygen degradation domain selectivity of the HIF prolyl hydroxylases. *Nat. Commun.* **2016,** *7*, 12673; (c) Epstein, A. C.; Gleadle, J. M.; McNeill, L. A.; Hewitson, K. S.; O'Rourke, J.; Mole, D. R.; Mukherji, M.; Metzen, E.; Wilson, M. I.; Dhanda, A.; Tian, Y. M.; Masson, N.; Hamilton, D. L.; Jaakkola, P.; Barstead, R.; Hodgkin, J.; Maxwell, P. H.; Pugh, C. W.; Schofield, C. J.; Ratcliffe, P. J. C. elegans EGL-9 and mammalian homologs define a family of dioxygenases that regulate HIF by prolyl hydroxylation. *Cell* **2001,** *107* (1), 43-54; (d) Hirsila, M.; Koivunen, P.; Gunzler, V.; Kivirikko, K. I.; Myllyharju, J. Characterization of the human prolyl 4-hydroxylases that modify the hypoxia-inducible factor. *J. Biol. Chem.* **2003,** *278* (33), 30772-30780; (e) Ivan, M.; Haberberger, T.; Gervasi, D. C.; Michelson, K. S.; Gunzler, V.; Kondo, K.; Yang, H.; Sorokina, I.; Conaway, R. C.; Conaway, J. W.; Kaelin, W. G., Jr. Biochemical purification and pharmacological inhibition of a mammalian prolyl hydroxylase acting on hypoxia-inducible factor. *Proc. Natl. Acad. Sci. U. S. A.* **2002,** *99* (21), 13459-13464; (f) Smirnova, N. A.; Hushpulian, D. M.; Speer, R. E.; Gaisina, I. N.; Ratan, R. R.; Gazaryan, I. G. Catalytic mechanism and substrate specificity of HIF prolyl hydroxylases. *Biochemistry (Moscow)* **2012,** *77* (10), 1108-1119.

7. (a) Robinson, A.; Keely, S.; Karhausen, J.; Gerich, M. E.; Furuta, G. T.; Colgan, S. P. Mucosal protection by hypoxia-inducible factor prolyl hydroxylase inhibition. *Gastroenterology* **2008,** *134* (1), 145-155; (b) Tambuwala, M. M.; Cummins, E. P.; Lenihan, C. R.; Kiss, J.; Stauch, M.; Scholz, C. C.; Fraisl, P.; Lasitschka, F.; Mollenhauer, M.; Saunders, S. P.; Maxwell, P. H.; Carmeliet, P.; Fallon, P. G.; Schneider, M.; Taylor, C. T. Loss of prolyl hydroxylase-1 protects against colitis through reduced epithelial cell apoptosis and increased barrier function.

Gastroenterology **2010,** *139* (6), 2093-2101; (c) Van Welden, S.; Laukens, D.; Ferdinande, L.; De Vos, M.; Hindryckx, P. Differential expression of prolyl hydroxylase 1 in patients with ulcerative colitis versus patients with Crohn's disease/infectious colitis and healthy controls. *J. Inflammation* **2013,** *10* (1), 36.

8. Bao, W.; Qin, P.; Needle, S.; Erickson-Miller, C. L.; Duffy, K. J.; Ariazi, J. L.; Zhao, S.; Olzinski, A. R.; Behm, D. J.; Pipes, G. C.; Jucker, B. M.; Hu, E.; Lepore, J. J.; Willette, R. N. Chronic inhibition of hypoxia-inducible factor prolyl 4-hydroxylase improves ventricular performance, remodeling, and vascularity after myocardial infarction in the rat. *J. Cardiovasc. Pharmacol.* **2010,** *56* (2), 147-155.

9. (a) Nangaku, M.; Izuhara, Y.; Takizawa, S.; Yamashita, T.; Fujii-Kuriyama, Y.; Ohneda, O.; Yamamoto, M.; van Ypersele de Strihou, C.; Hirayama, N.; Miyata, T. A novel class of prolyl hydroxylase inhibitors induces angiogenesis and exerts organ protection against ischemia. *Arterioscler. Thromb. Vasc. Biol.* **2007,** *27* (12), 2548-2554; (b) Karuppagounder, S. S.; Ratan, R. R. Hypoxia-inducible factor prolyl hydroxylase inhibition: robust new target or another big bust for stroke therapeutics? *J. Cereb. Blood Flow Metab.* **2012,** *32* (7), 1347-1361; (c) Kunze, R.; Zhou, W.; Veltkamp, R.; Wielockx, B.; Breier, G.; Marti, H. H. Neuron-specific prolyl-4-hydroxylase domain 2 knockout reduces brain injury after transient cerebral ischemia. *Stroke* **2012,** *43* (10), 2748-2756; (d) Ogle, M. E.; Gu, X.; Espinera, A. R.; Wei, L. Inhibition of prolyl hydroxylases by dimethyloxaloylglycine after stroke reduces ischemic brain injury and requires hypoxia inducible factor-1alpha. *Neurobiol. Dis.* **2012,** *45* (2), 733-742.

10. Schneider, M.; Van Geyte, K.; Fraisl, P.; Kiss, J.; Aragones, J.; Mazzone, M.; Mairbaurl, H.; De Bock, K.; Jeoung, N. H.; Mollenhauer, M.; Georgiadou, M.; Bishop, T.; Roncal, C.;

Sutherland, A.; Jordan, B.; Gallez, B.; Weitz, J.; Harris, R. A.; Maxwell, P.; Baes, M.; Ratcliffe, P.; Carmeliet, P. Loss or silencing of the PHD1 prolyl hydroxylase protects livers of mice against ischemia/reperfusion injury. *Gastroenterology* **2010,** *138* (3), 1143-1154 e1-2.

11. Bernhardt, W. M.; Campean, V.; Kany, S.; Jurgensen, J. S.; Weidemann, A.; Warnecke, C.; Arend, M.; Klaus, S.; Gunzler, V.; Amann, K.; Willam, C.; Wiesener, M. S.; Eckardt, K. U. Preconditional activation of hypoxia-inducible factors ameliorates ischemic acute renal failure. *J. Am. Soc. Nephrol.* **2006,** *17* (7), 1970-1978.

12. (a) Niatsetskaya, Z.; Basso, M.; Speer, R. E.; McConoughey, S. J.; Coppola, G.; Ma, T. C.; Ratan, R. R. HIF prolyl hydroxylase inhibitors prevent neuronal death induced by mitochondrial toxins: therapeutic implications for Huntington's disease and Alzheimer's disease. *Antioxid. Redox Signaling* **2010,** *12* (4), 435-443; (b) Rajagopalan, S.; Rane, A.; Chinta, S. J.; Andersen, J. K. Regulation of ATP13A2 via PHD2-HIF1alpha signaling is critical for cellular iron homeostasis: implications for Parkinson's disease. *J. Neurosci.* **2016,** *36* (4), 1086-1095; (c) Siddiq, A.; Aminova, L. R.; Ratan, R. R. Prolyl 4-hydroxylase activity-responsive transcription factors: from hydroxylation to gene expression and neuroprotection. *Front. Biosci.* **2008,** *13*, 2875-2887; (d) Siddiq, A.; Aminova, L. R.; Troy, C. M.; Suh, K.; Messer, Z.; Semenza, G. L.; Ratan, R. R. Selective inhibition of hypoxia-inducible factor (HIF) prolyl-hydroxylase 1 mediates neuroprotection against normoxic oxidative death via HIF- and CREB-independent pathways. *J. Neurosci.* **2009,** *29* (27), 8828-8838; (e) Siddiq, A.; Ayoub, I. A.; Chavez, J. C.; Aminova, L.; Shah, S.; LaManna, J. C.; Patton, S. M.; Connor, J. R.; Cherny, R. A.; Volitakis, I.; Bush, A. I.; Langsetmo, I.; Seeley, T.; Gunzler, V.; Ratan, R. R. Hypoxia-inducible factor prolyl 4-hydroxylase inhibition. A target for neuroprotection in the central nervous system. *J. Biol. Chem.* **2005,** *280* (50), 41732-41743; (f) Soucek, T.; Cumming, R.; Dargusch, R.; Maher, P.;

Schubert, D. The regulation of glucose metabolism by HIF-1 mediates a neuroprotective response to amyloid beta peptide. *Neuron* **2003,** *39* (1), 43-56.

13. Yan, L.; Colandrea, V. J.; Hale, J. J. Prolyl hydroxylase domain-containing protein inhibitors as stabilizers of hypoxia-inducible factor: small molecule-based therapeutics for anemia. *Expert. Opin. Ther. Pat.* **2010,** *20* (9), 1219-1245.

14. Harnoss, J. M.; Strowitzki, M. J.; Radhakrishnan, P.; Platzer, L. K.; Harnoss, J. C.; Hank, T.; Cai, J.; Ulrich, A.; Schneider, M. Therapeutic inhibition of prolyl hydroxylase domain-containing enzymes in surgery: putative applications and challenges. *Hypoxia* **2015,** *3*, 1-14.

15. (a) Kim, S. Y.; Yang, E. G. Recent advances in developing inhibitors for hypoxia-inducible factor prolyl hydroxylases and their therapeutic implications. *Molecules* **2015,** *20* (11), 20551-20568; (b) Rabinowitz, M. H. Inhibition of hypoxia-inducible factor prolyl hydroxylase domain oxygen sensors: tricking the body into mounting orchestrated survival and repair responses. *J. Med. Chem.* **2013,** *56* (23), 9369-9402; (c) Wu, Y.; Wang, N.; Lei, Y.; Hu, T.; You, Q.; Zhang, X. Small-molecule inhibitors of HIF-PHD2: a valid strategy to renal anemia treatment in clinical therapy. *Med. Chem. Commun.* **2016,** *7* (7), 1271-1284.

16. Arend, M.; Flippin, L.; Guenzler-Pukall, V.; Ho, W.-B.; Turtle, E.; Du, X. Novel nitrogen-containing heteroaryl compounds and methods of use thereof. US2004254215, 2004.

17. Kawamoto, R. M. Prolyl hydroxylase inhibitors and methods of use. US2007299086, 2007.

18. Thede, K.; Flamme, I.; Oehme, F.; Ergueden, J.-K.; Stoll, F.; Schuhmacher, J.; Wild, H.; Kolkhof, P.; Beck, H.; Keldenich, J.; Akbaba, M.; Jeske, M. Substituted dihydropyrazolones for treating cardiovascular and haematological diseases. WO2008067871, 2008.

19. Hopkins, A. L.; Groom, C. R.; Alex, A. Ligand efficiency: a useful metric for lead selection. *Drug Discovery Today* **2004,** *9* (10), 430-431.

20. Rankovic, Z. CNS drug design: balancing physicochemical properties for optimal brain exposure. *J. Med. Chem.* **2015,** *58* (6), 2584-2608.

21. Miyaura, N.; Yamada, K.; Suzuki, A. New stereospecific cross-coupling by the palladium-catalyzed reaction of 1-alkenylboranes with 1-alkenyl or 1-alkynyl halides. *Tetrahedron Lett.* **1979,** *20* (36), 3437-3440.

22. Milstein, D.; Stille, J. K. Palladium-catalyzed coupling of tetraorganotin compounds with aryl and benzyl halides - synthetic utility and mechanism. *J. Am. Chem. Soc.* **1979,** *101* (17), 4992-4998.

23. Polanc, S.; Vercek, B.; Sek, B.; Stanovnik, B.; Tisler, M. Heterocycles. CXVIII. Pyridazines. LXVI. Novel method of annelation of 1,2,4-triazole ring of N2-C3 bond to azines. *J. Org. Chem.* **1974,** *39* (15), 2143-2147.

24. (a) Guram, A. S.; Buchwald, S. L. Palladium-catalyzed aromatic aminations with in-situ generated aminostannanes. *J. Am. Chem. Soc.* **1994,** *116* (17), 7901-7902; (b) Paul, F.; Patt, J.; Hartwig, J. F. Palladium-catalyzed formation of carbon-nitrogen bonds - reaction intermediates and catalyst improvements in the hetero cross-coupling of aryl halides and tin amides. *J. Am. Chem. Soc.* **1994,** *116* (13), 5969-5970.

25. Yin, J. J.; Buchwald, S. L. Palladium-catalyzed intermolecular coupling of aryl halides and amides. *Org. Lett.* **2000,** *2* (8), 1101-1104.

Table of Contents graphic.